Int. J. Solids Structures, 1970, Vol. 6, pp. 699 to 724. Pergamon Press. Printed in Great Britain

A DIFFERENCE-BASED VARIATIONAL METHOD FOR SHELLS

DONALD E. JOHNSON

Avco Systems Division,
Wilmington, Massachusetts

Abstract—This paper describes a difference-based variational method for analyzing a general class of two dimensional shell problems, including shells with cutouts. The method is essentially an adaptation of the variational method for setting up difference operators. Results from two example problems are given and the effectiveness of the method is illustrated. Although the method has broader applicability, this work is limited to static linear elastic deformations of thin shells.

NOTATION

P	Potential energy of the shell
$N_{11}, N_{12}, N_{21}, N_{22}$	Stress resultants (Fig. 1b)
$\bar{N}_{12}$	Modified stress resultant
$M_{11}, M_{12}, M_{21}, M_{22}$	Stress couples (Fig. 1a)
$\bar{M}_{12}$	Modified stress couple
$\varepsilon_{11}, \varepsilon_{12}, \varepsilon_{22}$	Strains in middle surface
$\kappa_{11}, \kappa_{22}, \kappa_{12}, \kappa_{21}$	Bending and twisting strains
α_1, α_2	Coefficients in metric form of middle surface
ξ_1, ξ_2	Coordinates in principal curvature directions on middle surface of shell
$\underline{e}_1, \underline{e}_2, \underline{e}_n$	Unit vectors in directions 1, 2 and n, respectively (Fig. 1)
U_1, U_2, W	Displacement components in 1, 2 and n directions, respectively (Fig. 1)
$\underline{U}$	$= U_1\underline{e}_1 + U_2\underline{e}_2 + W\underline{e}_n$ vector displacement of shell middle surface
$\underline{f}$	$= f_1\underline{e}_1 + f_2\underline{e}_2 + f_n\underline{e}_n$ external vector force per unit area of shell middle surface
$\underline{N}$	$= N_1\underline{e}_1 + N_2\underline{e}_2 + N_n\underline{e}_n$ external vector force per unit length acting on boundary of shell
M_s	Externally applied moment per unit length, positive if directed in direction of increasing s
ϕ_1, ϕ_2, ϕ_n	Rotations (Fig. 1a)
ϕ_s	Component of rotation vector tangent to boundary and pointing in direction of increasing s
s, s^*	Path variables, along boundary of shell
$\hat{E}$	Modulus of elasticity
ν	Poisson's ratio
h	Thickness of shell

Remarks on notation

1. Other symbols, not listed above, are defined in the text.
2. Vectors are denoted by underlining.
3. Matrices are denoted by bold face type, with lower case bold face reserved for column matrices.
4. The transpose of a matrix is represented by the superscript T.

1. INTRODUCTION

THE variational method for setting up finite difference operators has been known for a long time. As early as 1928, Courant, Friedrichs and Lewy [1] used a variational procedure to derive finite difference expressions for the harmonic and biharmonic operators. In recent years, with the development in computers, there has been a renewed interest in this

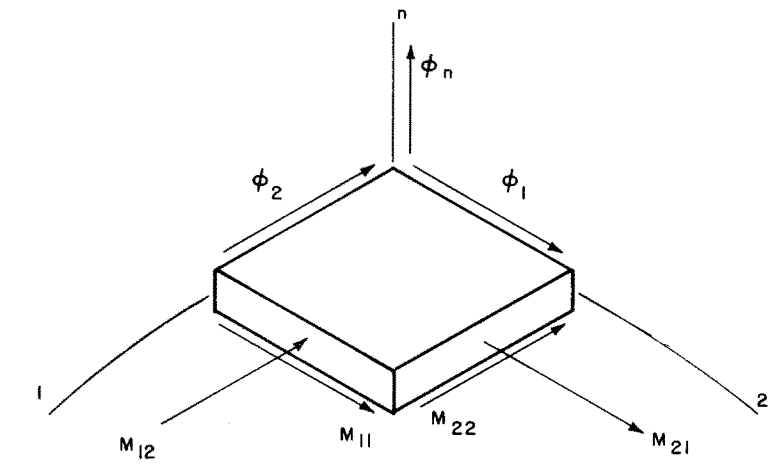

(a) STRESS COUPLES AND ROTATIONS

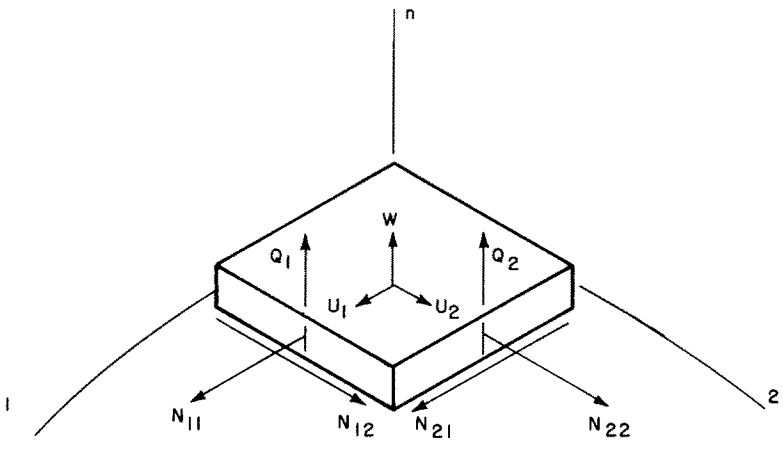

(b) STRESS RESULTANTS AND DISPLACEMENTS

FIG. 1. Orientation of coordinates, displacements, rotations, stress resultants and stress couples.

method [2–7]. The present method may be viewed as an extension of the variational method for setting up difference operators to the analysis of thin shells including such general two dimensional effects as shells with cutouts and arbitrarily curved boundaries. The two major innovations introduced in this work are: (1) development of a less restrictive scheme for positioning the discrete points at which unknown dependent variables are identified, and (2) development of a well organized scheme, particularly adapted for shells, of handling the geometry and computing the potential energy.

One of the features that this method has in common with the finite element method is the use of a variational principle. (Pertinent investigations of the two dimensional shell problem via the finite element method are described in references [8–11]). However, as may be seen from the development that follows, many features of this method, such as the choice of discrete variables and the method of evaluating integrals, are distinctly different from their finite element counterparts.

2. POTENTIAL ENERGY OF THE SHELL

The potential energy for a thin shell subjected to small linear elastic displacements may be written as follows by using Sanders' Theory [12]:

$$P = \int\int \tfrac{1}{2}(N_{11}\varepsilon_{11} + 2\bar{N}_{12}\varepsilon_{12} + N_{22}\varepsilon_{22} + M_{11}\kappa_{11} + 2\bar{M}_{12}\bar{\kappa}_{12} + M_{22}\kappa_{22})\alpha_1\alpha_2 \, d\xi_1 \, d\xi_2$$
$$- \int\int (\underline{f} \cdot \underline{U})\alpha_1\alpha_2 \, d\xi_1 \, d\xi_2 - \oint_{s^*} (\underline{N} \cdot \underline{U} + M_s\phi_s) \, ds^*. \tag{2.1}$$

The quantities appearing in equation (2.1) are identified in the Notation. The numerical subscripts appearing in the double integrals of equation (2.1) refer to the directions of principle curvature. The double integrations are extended over the area of the shell middle surface; the contour integration is extended along the shell boundary. (s^* is the path variable, defining the position along the shell boundary). Any contribution to the potential energy from the contour integral is caused by the presence of an external force $\underline{N}$ or external moment M_s applied to the shell boundary. The derivation of equation (2.1) presupposes that the portion of the boundary over which non-zero values of $\underline{N}$ or M_s are applied is a smooth curve without corners.

It is convenient at this stage to write equation (2.1) in a simpler form by introducing column matrices $\boldsymbol{\sigma}$ and $\boldsymbol{\varepsilon}$ representing generalized stress and strain as follows:

$$\boldsymbol{\sigma} = \begin{Bmatrix} N_{11} \\ N_{22} \\ 2\bar{N}_{12} \\ M_{11} \\ M_{22} \\ 2\bar{M}_{12} \end{Bmatrix} \qquad \boldsymbol{\varepsilon} = \begin{Bmatrix} \varepsilon_{11} \\ \varepsilon_{22} \\ \varepsilon_{12} \\ \kappa_{11} \\ \kappa_{22} \\ \bar{\kappa}_{12} \end{Bmatrix}. \tag{2.2}$$

Substitution of (2.2) into (2.1) leads to

$$P = \int\int \tfrac{1}{2}\boldsymbol{\sigma}^T\boldsymbol{\varepsilon}\alpha_1\alpha_2 \, dA - \int\int \underline{f} \cdot \underline{U}\alpha_1\alpha_2 \, dA$$
$$- \oint_s (\underline{N} \cdot \underline{U} + M_s\phi_s)\left(\frac{ds^*}{ds}\right) ds \tag{2.3}$$

where the elemental "area" in the ξ_1, ξ_2 plane, dA, given by

$$dA = d\xi_1 \, d\xi_2 \tag{2.4}$$

has been introduced. In addition, we have introduced in equation (2.3) a new path variable s, which indicates the position along the boundary as it appears in the ξ_1, ξ_2 plane.

We now divide the portion of the ξ_1, ξ_2 plane over which the double integration is extended into I areas, A_i, which are identified by the index i. A schematic example of this division is shown in Fig. 2, in which this portion of the ξ_1, ξ_2 plane has been divided into 24 areas ($I = 24$). In this example it is assumed that there are symmetries in the shell and the loading which allow the problem to be reduced to the treatment of the quarter panel as

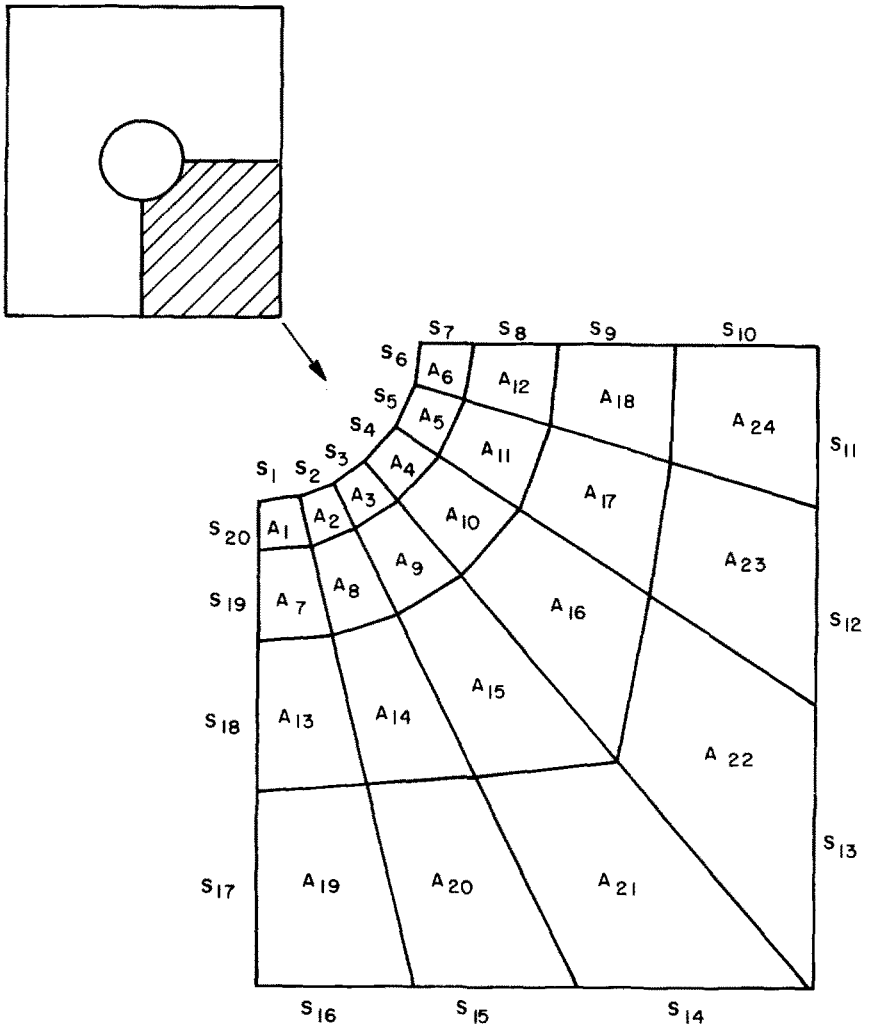

FIG. 2. Schematic example of division of ξ_1, ξ_2 plane into areas (rectangular panel with circular hole).

shown. A more detailed example of this type of problem is shown in Fig. 3. The terms in the integrands in equation (2.3) are functions of ξ_1 and ξ_2; let us denote $\boldsymbol{\sigma}, \boldsymbol{\varepsilon}, \underline{f}, \underline{U}, \alpha_1$ and α_2 evaluated at the centroid of each area A_i by the symbols $\boldsymbol{\sigma}_i, \boldsymbol{\varepsilon}_i, \underline{f}_i, \underline{U}_i, \alpha_{1_i}$ and α_{2_i} respectively. If $\boldsymbol{\sigma}, \boldsymbol{\varepsilon}, \underline{f}, \underline{U}, \alpha_1$ and α_2 are analytic functions, then by using the Taylor series expansions of $\boldsymbol{\sigma}, \boldsymbol{\varepsilon}, \underline{f}, \underline{U}, \alpha_1$ and α_2 about the centroid of each area A_i one can show that

$$\int\int \tfrac{1}{2}\boldsymbol{\sigma}^T\boldsymbol{\varepsilon}\alpha_1\alpha_2 \, dA = \sum_{i=1}^{I} \tfrac{1}{2}\boldsymbol{\sigma}_i^T\boldsymbol{\varepsilon}_i\alpha_{1_i}\alpha_{2_i}A_i + O(\Delta^2) \tag{2.5}$$

and

$$\int\int \underline{f} \cdot \underline{U}\alpha_1\alpha_2 \, dA = \sum_{i=1}^{I} \underline{f}_i \cdot \underline{U}_i\alpha_{1_i}\alpha_{2_i}A_i + O(\Delta^2) \tag{2.6}$$

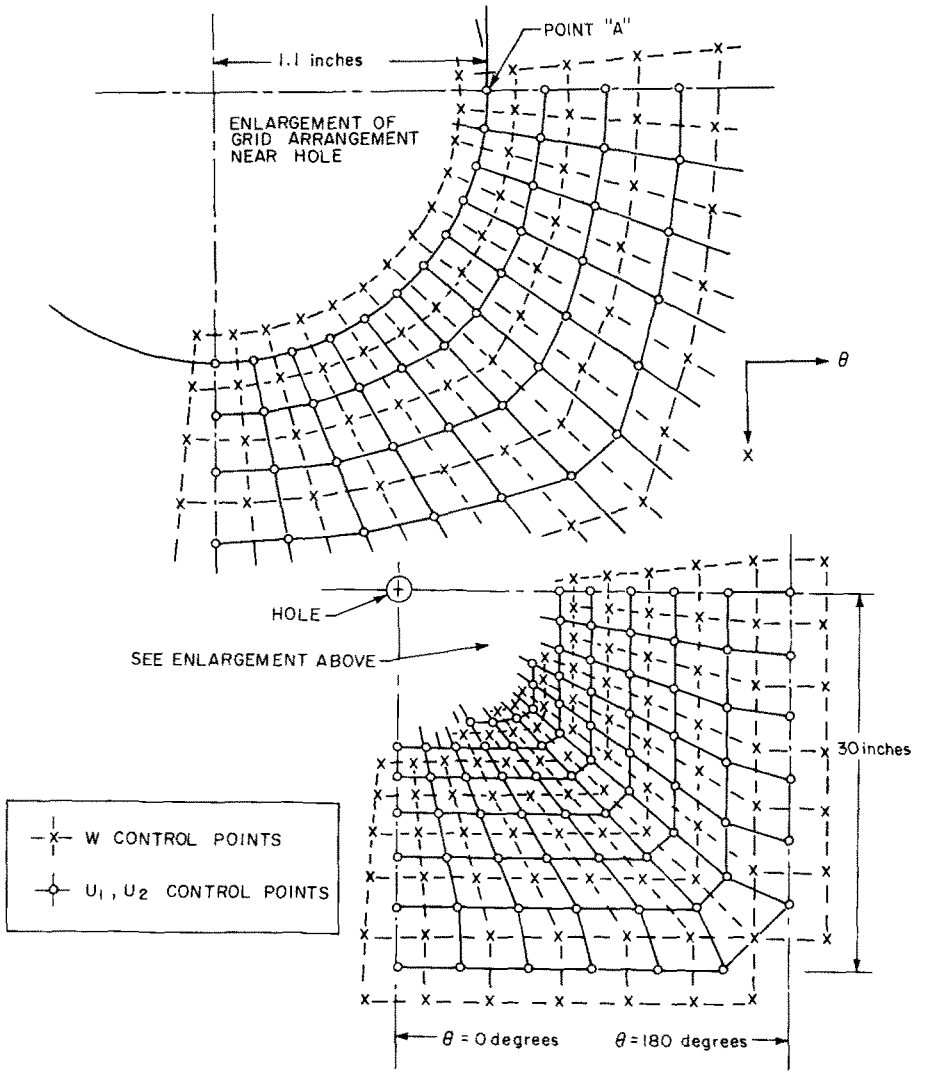

FIG. 3. Example of arrangement of control points: cylindrical shell with circular hole.

where $O(\Delta^2)$ is the order of error, Δ being the maximum dimension to be found in any of the areas A_i. It should be pointed out that if $\boldsymbol{\sigma}_i$, $\boldsymbol{\varepsilon}_i$, $\underline{f}_i$, $\underline{U}_i$, α_{1_i} and α_{2_i} were evaluated at any point other than the centroid of each area A_i, then the error in equations (2.5) and (2.6) would be of order Δ rather than Δ^2.

In a similar manner, by assuming $\underline{N}$, $\underline{U}$, M_s, ϕ_s and (ds*/ds) to be analytic functions of position along the boundary, the following may be written

$$\oint_s (\underline{N} \cdot \underline{U} + M_s\phi_s)\left(\frac{ds^*}{ds}\right) ds = \sum_{j=1}^{J} (\underline{N}_j \cdot \underline{U}_j + M_{s_j}\phi_{s_j})\left(\frac{ds^*}{ds}\right)_j s_j + O(\Delta^2) \tag{2.7}$$

where the symbols $\underline{N}_j$, $\underline{U}_j$, M_{s_j}, ϕ_{s_j} and $(\mathrm{ds}^*/\mathrm{ds})_j$ represent, analogously, the terms $\underline{N}$, $\underline{U}$, M_s, ϕ_s and $(\mathrm{ds}^*/\mathrm{ds})$ evaluated at the centroid of each line segment s_j. A schematic example showing the division of the shell boundary into various increments of length, s_j, is given in Fig. 2. [In the actual implementation of this method, curved boundaries are approximated by a sequence of chords. Consequently, the errors thus introduced, for smooth curves, are of order Δ^2, i.e. of the same order as shown in equation (2.7)].

Substitution of equations (2.5), (2.6) and (2.7) into equation (2.3) gives the following expression for the potential energy

$$P = \sum_{i=1}^{I} \tfrac{1}{2}\boldsymbol{\sigma}_i^T \boldsymbol{\varepsilon}_i \alpha_{1_i}\alpha_{2_i}A_i - \sum_{i=1}^{I} \underline{f}_i \cdot \underline{U}_i \alpha_{1_i}\alpha_{2_i}A_i - \sum_{j=1}^{J} (\underline{N}_j \cdot \underline{U}_j + M_{s_j}\phi_{s_j})\left(\frac{\mathrm{ds}^*}{\mathrm{ds}}\right)_j s_j + O(\Delta^2). \tag{2.8}$$

The generalized elastic stress–strain laws may be written for each centroidal point as follows

$$\boldsymbol{\sigma}_i = \mathbf{C}_i \boldsymbol{\varepsilon}_i. \tag{2.9}$$

Depending on the specification of the elements of the matrix $\mathbf{C}_i$, the shell may be single-layered, multilayered, isotropic, anisotropic, etc. For example the elements of $\mathbf{C}_i$ for an isotropic single-layered shell, obtained from Sanders' theory [12], are given by

$$\mathbf{C}_i = \frac{\hat{E}h}{(1-\nu^2)} \begin{bmatrix} 1 & \nu & 0 & 0 & 0 & 0 \\ \nu & 1 & 0 & 0 & 0 & 0 \\ 0 & 0 & 2(1-\nu) & 0 & 0 & 0 \\ 0 & 0 & 0 & \dfrac{h^2}{12} & \dfrac{\nu h^2}{12} & 0 \\ 0 & 0 & 0 & \dfrac{\nu h^2}{12} & \dfrac{h^2}{12} & 0 \\ 0 & 0 & 0 & 0 & 0 & \dfrac{(1-\nu)h^2}{6} \end{bmatrix}. \tag{2.10}$$

Substitution of equation (2.9) into equation (2.8) gives

$$P = \sum_{i=1}^{I} \tfrac{1}{2}\boldsymbol{\varepsilon}_i^T \mathbf{C}_i^T \boldsymbol{\varepsilon}_i \alpha_{1_i}\alpha_{2_i}A_i - \sum_{i=1}^{I} \underline{f}_i \cdot \underline{U}_i \alpha_{1_i}\alpha_{2_i}A_i - \sum_{j=1}^{J} (\underline{N}_j \cdot \underline{U}_j + M_{s_j}\phi_{s_j})\left(\frac{\mathrm{ds}^*}{\mathrm{ds}}\right)_j s_j + O(\Delta^2). \tag{2.11}$$

Before proceeding further, it is convenient to represent equation (2.11) entirely in matrix form. This is accomplished by introducing various matrices defined as follows:

$$\boldsymbol{\varepsilon}^T = [\boldsymbol{\varepsilon}_1^T, \boldsymbol{\varepsilon}_2^T, \ldots, \boldsymbol{\varepsilon}_I^T] \tag{2.12}$$

$$\mathbf{E} = \begin{pmatrix} \mathbf{C}_1 & 0 & \cdots & 0 \\ 0 & \mathbf{C}_2 & \cdots & 0 \\ \cdots & \cdots & \cdots & \cdots \\ 0 & 0 & \cdots & \mathbf{C}_I \end{pmatrix} \tag{2.13}$$

$$\mathbf{g}^T = [\underline{f}_1 \cdot \underline{e}_{1,1}, \underline{f}_1 \cdot \underline{e}_{1,2}, \underline{f}_1 \cdot \underline{e}_{1,n}, \underline{f}_2 \cdot \underline{e}_{2,1}, \underline{f}_2 \cdot \underline{e}_{2,2}, \underline{f}_2 \cdot \underline{e}_{2,n}, \ldots, \underline{f}_I \cdot \underline{e}_{I,1}, \underline{f}_I \cdot \underline{e}_{I,2}, \underline{f}_I \cdot \underline{e}_{I,n}]$$

$$\mathbf{b}^T = [\underline{N}_1 \cdot \hat{\underline{e}}_{1,1}, \underline{N}_1 \cdot \hat{\underline{e}}_{1,2}, \underline{N}_1 \cdot \hat{\underline{e}}_{1,n}, \underline{N}_2 \cdot \hat{\underline{e}}_{2,1}, \underline{N}_2 \cdot \hat{\underline{e}}_{2,2}, \underline{N}_2 \cdot \hat{\underline{e}}_{2,n}, \ldots, \tag{2.14}$$

$$\underline{N}_J \cdot \hat{\underline{e}}_{J,1}, \underline{N}_J \cdot \hat{\underline{e}}_{J,2}, \underline{N}_J \cdot \hat{\underline{e}}_{J,n}] \tag{2.15}$$

$$\boldsymbol{\mu}^T = [M_{s_1}, M_{s_2}, \ldots, M_{s_J}]. \tag{2.16}$$

In equation (2.14), $\underline{e}_{i,1}, \underline{e}_{i,2}, \underline{e}_{i,n}$ are the unit vectors $\underline{e}_1, \underline{e}_2, \underline{e}_n$ evaluated at the centroid of A_i. In equation (2.15), $\hat{\underline{e}}_{j,1}, \hat{\underline{e}}_{j,2}, \hat{\underline{e}}_{j,n}$ are the unit vectors $\underline{e}_1, \underline{e}_2, \underline{e}_n$ evaluated at the center of length s_j. The length matrix $\mathbf{S}$ is a diagonal matrix with the following elements on the diagonal

$$\tilde{s}_1, \tilde{s}_1, \tilde{s}_1, \tilde{s}_2, \tilde{s}_2, \tilde{s}_2, \ldots, \tilde{s}_J, \tilde{s}_J, \tilde{s}_J$$

where

$$\tilde{s}_j = (\mathrm{d}s^*/\mathrm{d}s)_j s_j \quad \text{for } j = 1, 2, \ldots, J.$$

The length matrix $\boldsymbol{\Lambda}$ is a diagonal matrix with the following elements on the diagonal

$$\tilde{s}_1, \tilde{s}_2, \tilde{s}_3, \ldots, \tilde{s}_J.$$

The area matrix $\boldsymbol{\Omega}$ is a diagonal matrix with the following elements on the diagonal

$$\tilde{A}_1, \tilde{A}_1, \tilde{A}_1, \tilde{A}_2, \tilde{A}_2, \tilde{A}_2, \ldots, \tilde{A}_I, \tilde{A}_I, \tilde{A}_I$$

where

$$\tilde{A}_i = \alpha_{1_i} \alpha_{2_i} A_i \quad \text{for } i = 1, 2, \ldots, I.$$

The definition of the area matrix $\mathbf{A}$ may be obtained from equation (2.13) by replacing $\mathbf{C}_i$ (for $i = 1, 2, \ldots, I$) by $\tilde{A}_i \hat{\mathbf{I}}$ (where $\hat{\mathbf{I}}$ is a 6×6 identity matrix) and by replacing $\mathbf{E}$ by $\mathbf{A}$. The definition of column matrix $\mathbf{d}$ may be obtained from equation (2.14) by replacing $\underline{f}_i$ (for $i = 1, 2, \ldots, I$) by $\underline{U}_i$ and $\mathbf{g}$ by $\mathbf{d}$; the column matrix $\mathbf{a}$ from equation (2.15) by replacing $\underline{N}_j$ (for $j = 1, 2, \ldots, J$) by $\underline{U}_j$ and $\mathbf{b}$ by $\mathbf{a}$; and the column matrix $\boldsymbol{\psi}$ from equation (2.16) by replacing M_{s_j} (for $j = 1, 2, \ldots, J$) by ϕ_{s_j} and $\boldsymbol{\mu}$ by $\boldsymbol{\psi}$.

To further clarify the matrix representations a summary of matrix sizes is given in Table 1.

TABLE 1. SUMMARY OF MATRIX SIZES

Matrices	$\mathbf{e}$	$\mathbf{g}, \mathbf{d}$	$\mathbf{b}, \mathbf{a}$	$\boldsymbol{\mu}, \boldsymbol{\psi}$	$\mathbf{E}, \mathbf{A}$	$\boldsymbol{\Omega}$	$\mathbf{S}$	$\boldsymbol{\Lambda}$
No. of rows	$6I$	$3I$	$3J$	J	$6I$	$3I$	$3J$	J
No. of columns	1	1	1	1	$6I$	$3I$	$3J$	J

By using the newly defined matrices $\mathbf{e}, \mathbf{g}, \mathbf{d}, \mathbf{b}, \mathbf{a}, \boldsymbol{\mu}, \boldsymbol{\psi}, \mathbf{E}, \mathbf{A}, \boldsymbol{\Omega}, \mathbf{S}$ and $\boldsymbol{\Lambda}$, equation (2.11) becomes

$$P = \tfrac{1}{2}\mathbf{e}^T\mathbf{E}^T\mathbf{A}\mathbf{e} - \mathbf{g}^T\boldsymbol{\Omega}\mathbf{d} - \mathbf{b}^T\mathbf{S}\mathbf{a} - \boldsymbol{\mu}^T\boldsymbol{\Lambda}\boldsymbol{\psi} + O(\Delta^2) \tag{2.17}$$

In the present method we consider the discrete values of the displacement components U_1, U_2 and W at a finite number of distinct "control" points. A more precise description of just how these control points are selected for each of the displacement components will be deferred to a later section of this paper. At this stage in the derivation we shall merely assume that a total number of K values of the displacement components are assigned to various control points, and that each of these K values may be uniquely identified by the symbol u_k, where $k = 1, 2, \ldots,$ or K. Thus a column matrix $\mathbf{u}$ representing the displacement may be defined as follows

$$\mathbf{u} = \begin{Bmatrix} u_1 \\ u_2 \\ \vdots \\ u_K \end{Bmatrix}. \tag{2.18}$$

The next step is to construct generalized strain–displacement relations that relate each of the elements of the strain matrix $\mathbf{e}$ to elements of the displacement matrix $\mathbf{u}$. These generalized strain–displacement relations to be constructed are discrete variable representations of the strain–displacement relations for the continuum, which have been given by Sanders [12] as follows:

$$\begin{aligned}
\varepsilon_{11} &= \frac{1}{\alpha_1}\frac{\partial U_1}{\partial \xi_1} + \frac{1}{\alpha_1\alpha_2}\frac{\partial \alpha_1}{\partial \xi_2}U_2 + \frac{W}{R_1} \\
\varepsilon_{22} &= \frac{1}{\alpha_2}\frac{\partial U_2}{\partial \xi_2} + \frac{1}{\alpha_1\alpha_2}\frac{\partial \alpha_2}{\partial \xi_1}U_1 + \frac{W}{R_2} \\
\varepsilon_{12} &= \frac{1}{2\alpha_1\alpha_2}\left(\alpha_2\frac{\partial U_2}{\partial \xi_1} + \alpha_1\frac{\partial U_1}{\partial \xi_2} - \frac{\partial \alpha_1}{\partial \xi_2}U_1 - \frac{\partial \alpha_2}{\partial \xi_1}U_2\right) \\
\kappa_{11} &= \frac{1}{\alpha_1}\frac{\partial \phi_1}{\partial \xi_1} + \frac{1}{\alpha_1\alpha_2}\frac{\partial \alpha_1}{\partial \xi_2}\phi_2 \\
\kappa_{22} &= \frac{1}{\alpha_2}\frac{\partial \phi_2}{\partial \xi_2} + \frac{1}{\alpha_1\alpha_2}\frac{\partial \alpha_2}{\partial \xi_1}\phi_1 \\
\bar{\kappa}_{12} &= \frac{1}{2\alpha_1\alpha_2}\left[\alpha_2\frac{\partial \phi_2}{\partial \xi_1} + \alpha_1\frac{\partial \phi_1}{\partial \xi_2} - \frac{\partial \alpha_1}{\partial \xi_2}\phi_1 - \frac{\partial \alpha_2}{\partial \xi_1}\phi_2\right. \\
&\quad \left. + \frac{1}{2}\left(\frac{1}{R_2} - \frac{1}{R_1}\right)\left(\frac{\partial \alpha_2 U_2}{\partial \xi_1} - \frac{\partial \alpha_1 U_1}{\partial \xi_2}\right)\right]
\end{aligned} \tag{2.19}$$

where

$$\begin{aligned}
\phi_1 &= \frac{U_1}{R_1} - \frac{1}{\alpha_1}\frac{\partial W}{\partial \xi_1} \\
\phi_2 &= \frac{U_2}{R_2} - \frac{1}{\alpha_2}\frac{\partial W}{\partial \xi_2}.
\end{aligned} \tag{2.20}$$

The construction of these discrete variable generalized strain–displacement relations from the relations for the continuum (2.19), (2.20) will naturally involve some type of interpolative scheme and a truncation error. Since the description of the selection and positioning of the control points has been deferred to a later section of this paper, and since many different interpolative schemes could be chosen, a more detailed discussion of the generalized strain–displacement relations is also deferred to a later section. Thus for the present we assume that generalized strain–displacement relations having a truncation error of order Δ or Δ^2 can be constructed and represented in the following matrix form:

$$\mathbf{e} = \mathbf{Lu} + O(\Delta^n) \qquad n = 1 \text{ or } 2. \tag{2.21}$$

In a similar manner, we assume that an interpolative scheme has been used to express the displacement components and the rotation on the boundary in terms of the values of u_k at the control points:

$$\left.\begin{aligned} \mathbf{d} &= \mathbf{Du} + O(\Delta^n) && \text{(2.22a)} \\ \mathbf{a} &= \mathbf{Qu} + O(\Delta^n) && \text{(2.22b)} \\ \boldsymbol{\psi} &= \mathbf{Hu} + O(\Delta^n) && \text{(2.22c)} \end{aligned}\right\} \quad n = 1 \text{ or } 2.$$

Substitution of equations (2.21) and (2.22) into equation (2.17) gives

$$\begin{aligned} P = {} & \tfrac{1}{2}\mathbf{u}^T(\mathbf{L}^T\mathbf{E}^T\mathbf{AL})\mathbf{u} \\ & -(\mathbf{g}^T\boldsymbol{\Omega}\mathbf{D} + \mathbf{b}^T\mathbf{SQ} + \boldsymbol{\mu}^T\boldsymbol{\Lambda}\mathbf{H})\mathbf{u} + O(\Delta^n) \qquad n = 1 \text{ or } 2. \end{aligned} \tag{2.23}$$

It should be pointed out that, because of the sparseness of the matrices **L**, **D**, **Q** and **H**, no cumulative lowering of the order of error occurs during the matrix multiplications when equations (2.21) and (2.22) are substituted into equation (2.17). The sparseness of the matrices **L**, **D**, **Q** and **H** is primarily due to the nature of the interpolation schemes, which are described in Section 4.

3. MINIMIZATION OF POTENTIAL ENERGY

The next step is to determine the vector **u** that both minimizes the potential energy P in equation (2.23) and, at the same time, satisfies any constraints that may be introduced by displacement-type boundary conditions. These constraints are introduced if values of U_1, U_2, W or ϕ_s are specified in lieu of N_1, N_2, N_n or M_s, respectively, at any point on the boundary.

Two methods of handling the minimization process when constraints are involved are: (1) reduction of the number of unknowns before minimization, and (2) use of Lagrange multipliers. In this work we use the former method because of its computational advantages. Although a description of the choice of control points has been deferred to Section 4, nevertheless we shall presently outline the method of reducing the number of unknowns. We suppose that values of U_1, U_2, W and/or ϕ_s have been specified along certain portions of the shell boundaries. By using appropriate interpolation formulas (see Section 4) we can write algebraic relations that represent these displacement boundary conditions at various points along the boundary. These algebraic relations are then cast into the following matrix form

$$\mathbf{u}_b = \mathbf{Gu}_a + \mathbf{r} + O(\Delta^2) \tag{3.1}$$

where $\mathbf{u}_a$, and $\mathbf{u}_b$ are partitioned forms of the displacement vector $\mathbf{u}$, given by

$$\mathbf{u} = \begin{Bmatrix} \mathbf{u}_a \\ \cdots \\ \mathbf{u}_b \end{Bmatrix}. \tag{3.2}$$

The number of elements in $\mathbf{u}_a$ is denoted by $\hat{K}$; the number of elements in $\mathbf{u}$ was previously denoted by K. Consequently, we are reducing the number of unknowns from K to $\hat{K}$ by introducing the $K-\hat{K}$ constraints specified by equation (3.1). Hence equation (3.1) is used to eliminate $\mathbf{u}_b$ from matrix equation (2.23). The result of this elimination, after some matrix manipulation, is:

$$P = P_0(\mathbf{u}_a) + O(\Delta^n) \qquad n = 1 \text{ or } 2 \tag{3.3}$$

where

$$\begin{aligned}
P_0(\mathbf{u}_a) &= \tfrac{1}{2}\mathbf{u}_a^T(\hat{\mathbf{L}}^T\mathbf{E}^T\mathbf{A}\hat{\mathbf{L}})\mathbf{u}_a + \boldsymbol{\gamma}^T\mathbf{u}_a + \boldsymbol{\rho} \\
\boldsymbol{\gamma}^T &= [\tfrac{1}{2}\mathbf{L}_b\mathbf{r}^T(\mathbf{E}^T\mathbf{A} + \mathbf{A}^T\mathbf{E})\hat{\mathbf{L}} - \mathbf{g}^T\boldsymbol{\Omega}\hat{\mathbf{D}} - \mathbf{b}^T\mathbf{S}\hat{\mathbf{Q}} - \boldsymbol{\mu}^T\boldsymbol{\Lambda}\hat{\mathbf{H}}]\mathbf{u}_a \\
\boldsymbol{\rho} &= [\tfrac{1}{2}(\mathbf{L}_b\mathbf{r})^T\mathbf{E}^T\mathbf{L}_b - \mathbf{g}^T\boldsymbol{\Omega}\mathbf{D}_b - \mathbf{b}\mathbf{S}\mathbf{Q}_b - \boldsymbol{\mu}^T\boldsymbol{\Lambda}\mathbf{H}_b]\mathbf{r} \\
\hat{\mathbf{L}} &= \mathbf{L}_a + \mathbf{L}_b\mathbf{G} \\
\hat{\mathbf{D}} &= \mathbf{D}_a + \mathbf{D}_b\mathbf{G} \\
\hat{\mathbf{Q}} &= \mathbf{Q}_a + \mathbf{Q}_b\mathbf{G} \\
\hat{\mathbf{H}} &= \mathbf{H}_a + \mathbf{H}_b\mathbf{G}
\end{aligned} \tag{3.4}$$

and $\mathbf{L}_a, \mathbf{L}_b, \mathbf{D}_a, \mathbf{D}_b, \mathbf{Q}_a, \mathbf{Q}_b, \mathbf{H}_a$ and $\mathbf{H}_b$ are the partitioned forms of $\mathbf{L}, \mathbf{D}, \mathbf{Q}$ and $\mathbf{H}$ respectively, as given in the following for $\mathbf{L}$

$$\mathbf{L} = [\mathbf{L}_a \vdots \mathbf{L}_b]$$

where $\mathbf{L}_a$ contains $\hat{K}$ columns, and $\mathbf{L}_b$ contains $K-\hat{K}$ columns.

Now that the $K-\hat{K}$ unknowns associated with the constraints have been eliminated, we can directly minimize the quantity $P_0(\mathbf{u}_a)$ in equation (3.3) by successively differentiating $P_0(\mathbf{u}_a)$ with respect to each of the $\hat{K}$ elements, u_k, of the vector $\mathbf{u}_a$. The resulting set of linear algebraic equations can be expressed in the following matrix form.

$$\mathbf{K}\mathbf{u}_a - \boldsymbol{\gamma} = 0 \tag{3.5}$$

where

$$\mathbf{K} = \tfrac{1}{2}\hat{\mathbf{L}}^T(\mathbf{E} + \mathbf{E}^T)\mathbf{A}\hat{\mathbf{L}}. \tag{3.6}$$

For a given finite number of unknowns $\hat{K}$, the solution, $\mathbf{u}_a$, of equation (3.5) will provide a minimum value of the quantity $P_0(\mathbf{u}_a)$. If, as the number of unknowns $\hat{K}$ is increased (and Δ thereby decreased), the discrete solution $\mathbf{u}_a$ converges to a continuous solution with the analytic properties assumed in the derivation, then in the limit as $\Delta \to 0$ the solution $\mathbf{u}_a$ will also provide a minimum value of the total potential energy P. Under these conditions the solution obtained in the limit will also satisfy the appropriate Euler equations associated with the potential energy for the continuum as expressed in equation (2.1). (Somewhat analogous observations concerning the convergence of the finite element method have been made by Tong and Pian [13]). Thus we see that the situation with respect to convergence is very similar to that usually found in solving differential equations by the

method of finite differences: namely, that if in the limit as $\Delta \to 0$ the numerical solution approaches a solution which has the necessary analytic properties, then in the limit the numerical solution satisfies the differential equation.

In spite of a similarity in form, equation (3.5) is distinctly different from the analogous equations obtained by applying the finite element method to shells [8–11]. The complete absence of unknown rotation quantities from the vector $\mathbf{u}_a$ clearly distinguishes equation (3.5) from its finite element counterparts.

Let us now briefly consider several characteristics of the **K** matrix. First, by taking the transpose of equation (3.6) it can be shown that the matrix **K** is symmetric. This fact is of considerable value from a computational point of view and was utilized in computing the results subsequently shown. Secondly, the existence of an elastic potential for the shell material leads to a symmetric **E** matrix and, consequently, equation (3.5) is identical to the matrix equation that would have been obtained if instead of using the theory of minimum potential energy we had used the analogous principle of virtual work. Thirdly, although we can show that the matrix **K** generated by this method for the general shell is *positive semidefinite*, the question of whether the matrix **K** is also *positive definite* is, for the general case, presently unresolved. (Positive definiteness requires that $\mathbf{u}_a^T\mathbf{K}\mathbf{u}_a > 0$ for any nonzero $\mathbf{u}_a$; positive semidefiniteness requires that $\mathbf{u}_a^T\mathbf{K}\mathbf{u}_a \geq 0$ for any nonzero $\mathbf{u}_a$). In this method any nonzero strain vector produces a positive strain energy. Consequently $\mathbf{u}_a^T\mathbf{K}\mathbf{u}_a > 0$ unless all elements of the vector **e** equal zero, thus assuring the positive semidefiniteness of **K**. The matrix **K** will also be positive definite if $\mathbf{e} = 0$ also implies that $\mathbf{u}_a = 0$. Thus a resolution of the question of positive definiteness involves a study of the matrix **L** (which relates **e** to **u**) and consideration of the constraints required to prevent rigid body displacements of the entire shell. Although it has been possible to prove the positive definiteness of the matrix **K** for a variety of flat plate problems (including both plane stress and bending†), a more general proof is not currently available. Additional (but nonconclusive) evidence of positive definiteness lies in the fact that no numerical difficulties have been experienced in solving the matrix equations (3.5). (If $\mathbf{e} = 0$ for some nonzero $\mathbf{u}_a$, then **K** will be singular). Finally, the band width of the matrix **K** is also of importance. As in the finite element method, the shell problem generates a substantially greater band width than the corresponding plane stress problem: in this method the band width of the matrix **K** for shells is essentially three times greater (for a large rectangular grid) than for the corresponding plane stress problem. A comparison of band widths with those generated by the finite element method is included in Section 6.

4. CONTROL POINTS, AREAS AND INTERPOLATIONS

4.1 *General*

In order to utilize the variational method described in this paper it is necessary to carry out the three following tasks: (1) the establishment of control points and the assignment of unknowns to these control points, (2) the subdivision of the ξ_1, ξ_2 plane into areas, A_i, and (3) the development and use of interpolation schemes for computing the strains, rotations and displacements in terms of the discrete unknowns, u_k. These tasks are highly interrelated; consequently their treatment has been deferred to this section where they can

† The assumption that the matrices $(\mathbf{I}-\hat{\mathbf{B}})$ are not singular is used. (See equation (4.17) and Section 4).

be treated together. An efficient and consistent method for accomplishing these three tasks is presented in this section.

The method presented here is based upon a grid of points which forms a set of non-uniform quadrilaterals. The method could quite easily be generalized so as to utilize figures other than quadrilaterals, but, as may be seen from the examples, the present method is sufficiently flexible for the effective treatment of a variety of shell boundary shapes, including cut-out problems.

4.2 *Control points and areas*

The positioning of control points for a typical example problem (a cylindrical shell with a circular hole) is shown in Fig. 3. (In this problem, $\xi_1 = x$, $\xi_2 = \theta$.) Two types of control points are shown in Fig. 3: "W Control Points" identified by the symbol X, and "U_1, U_2 Control Points" identified by the symbol O. Associated with each W Control Point is a discrete unknown value of the displacement component W; associated with each U_1, U_2 Control Point is one discrete unknown value of each of the displacement components U_1 and U_2. The idea of using one set of control points for the discrete values of one unknown variable and another set of control points for the discrete values of another unknown variable is not without precedent. In this work, the use of separate sets of control points for W and for U_1 and U_2 leads to greater compactness and, generally, to greater accuracy.

In Fig. 3 adjacent W Control Points are connected by straight lines (dashed) so as to form a set of quadrilaterals. The U_1, U_2 Control Points are located at the centroid of each of these quadrilaterals. Similarly, in Fig. 3 adjacent U_1, U_2 Control Points are connected by straight lines (solid) so as to form another set of quadrilaterals. This latter set of quadrilaterals define the areas A_i previously mentioned in Section 2. In addition, as shown in Fig. 3, a row of U_1, U_2 Control Points is positioned so as to fall on the shell boundary, so that all of the areas A_i fall within the boundaries of the shell. The computer code developed to implement this method provides for automatic mesh generation in which the Control Points may be automatically positioned so as to provide a smoothly varying grid properly fitted along the boundaries, i.e. the type of grid seen in Fig. 3.

4.3 *Interpolation*

Let us now consider the interpolative scheme used to compute the strains, rotations and displacements in terms of the discrete unknowns, u_k. First, we shall consider the scheme used to compute the elements of the matrix $\mathbf{L}$ of equation (2.21), i.e. to compute the discrete variable generalized stress–strain relations. To construct the matrix $\mathbf{L}$, it is necessary to express the strains at the centroid of each area A_i as a linear combination of the discrete unknowns, u_k. Since the values of α_1, α_2, R_1 and R_2 are, for any given shell, known functions of the coordinates ξ_1 and ξ_2, one can see from equations (2.19) and (2.20) that the interpolative portion of this task involves expressing the quantities U_1, U_2, W,

$$\frac{\partial U_1}{\partial \xi_1}, \quad \frac{\partial U_1}{\partial \xi_2}, \quad \frac{\partial U_2}{\partial \xi_1}, \quad \frac{\partial U_2}{\partial \xi_2}, \quad \frac{\partial W}{\partial \xi_1}, \quad \frac{\partial W}{\partial \xi_2}, \quad \frac{\partial^2 W}{\partial \xi_1^2}, \quad \frac{\partial^2 W}{\partial \xi_2^2},$$

and $(\partial^2 W)/(\partial \xi_1 \partial \xi_2)$ at the centroid of each area A_i as a linear combination of the discrete unknowns. In the paragraphs that follow, the interpolative schemes used to construct the discrete representations of each of the quantities listed above are described.

Before proceeding further we should briefly consider an alternative method for irregular meshes, which is described by Forsythe and Wasow [2], and also by Collatz [14]. Basically, this method involves expanding the function in a Taylor Series and the utilization of 5 or 6 control points. There are several disadvantages of this alternative method which render it unsuitable for the present work. The major disadvantage is that the method "breaks down" for various point arrangements. Collatz [14] shows that for certain point arrangements the matrix of coefficients is singular and only 5 points are required. Even for the case of uniform rectangular quadrilaterals the problem of selecting 6 points for which the matrix of coefficients is not singular proves to be not a simple task. [For example, the harmless looking set of six points (x, y) given by $(0, 0)$, $(0, \Delta)$, $(0, -\Delta)$, $(\Delta, 0)$, (Δ, Δ) and $(\Delta, -\Delta)$ leads to a singular coefficient matrix.] Although it appears possible in each of these cases to specially modify the algorithm and the selection of control points, the general usefulness of the method for automatic computer calculations is impaired. The method subsequently presented (for both first and second derivatives) provides a uniform procedure for selecting control points, does not require special treatment of exceptions and is particularly well-suited for automatic computer calculations of the derivatives. It should be pointed out that the method of interpolation used to compute the matrix **L** is the same for all areas A_i, i.e. no special exceptions (as are found, for example, in references [15] and [16]) are required for the areas A_i adjacent to the boundaries.

4.4 U_1, U_2 *and their derivatives*

The first derivatives of U_1 and U_2 at the centroid of each area A_i are obtained by writing Green's Theorem† for each area A_i:

$$\begin{aligned} \int\int_{A_i} \frac{\partial U_1}{\partial \xi_1} \, d\xi_1 \, d\xi_2 &= \oint_C U_1 \, d\xi_2 \\ \int\int_{A_i} \frac{\partial U_1}{\partial \xi_2} \, d\xi_1 \, d\xi_2 &= -\oint_C U_1 \, d\xi_1 \end{aligned} \tag{4.1}$$

and the analogous equations involving U_2. In equations (4.1) the integrals on the left hand side are area integrals extending over each quadrilateral area A_i; the integrals on the right hand side are contour integrals extending along the perimeter of each quadrilateral area A_i. In the next step the integrands of the area integrals on the left hand sides of (4.1) are approximated by their values at the centroid of A_i and consequently one can solve for the value of the first derivatives of U_1 at each centroid and obtain

$$\begin{aligned} \left(\frac{\partial U_1}{\partial \xi_1}\right)_i &= \frac{1}{A_i} \oint_C U_1 \, d\xi_2 + O(\Delta^2) \\ \left(\frac{\partial U_1}{\partial \xi_2}\right)_i &= -\frac{1}{A_i} \oint_C U_1 \, d\xi_1 + O(\Delta^2) \end{aligned} \tag{4.2}$$

and the analogous equations involving U_2. As in previous sections, the symbol Δ is used to denote the maximum dimension to be found in the area A_i. The centroidal approximation made in deriving equations (4.2) is analogous to the centroidal approximation previously

† Use of Green's Theorem in the derivation of difference equations is also described by Griffin and Varga [17] and Varga [18].

made in deriving equations (2.5), (2.6) and (2.7) in Section 2; consequently, the same order of error, $O(\Delta^2)$, is involved. Next, in order to obtain the desired algebraic relations from equations (4.2) the integrands of the contour integrals appearing in equations (4.2) are approximated by assuming U_1 (or U_2) to vary linearly between control points. The error thus introduced into the algebraic expressions for the first derivatives of U_1 and U_2 then becomes of order Δ, because although the approximations to the contour integrals involve errors of order Δ^3, the area A_i in the denominator is itself proportional to Δ^2. The fact that the assumed linear variation of U_1 (or U_2) in the contour integral lowers the order of error from Δ^2 to Δ is subsequently considered in greater detail in connection with the evaluation of the second derivatives of W. It should be pointed out that when the area identified by A_i is a parallelogram, the error in the algebraic expression for the first derivative becomes of order Δ^2. Furthermore, since the derivatives are thus expressed in terms of values of U_1 (or U_2) at four adjacent control points, a high degree of compactness and accuracy are achieved.

Once the discrete variable approximations to the first derivatives of U_1 and U_2 have been established, the problem of interpolating U_1 and U_2 may be greatly simplified. Values of U_1 and U_2 at the centroid of each area A_i can be obtained to order Δ^2 by expanding U_1 and U_2 about each centroid in a Taylor series (retaining only terms constant and linear in ξ_1 and ξ_2) and then utilizing the previously obtained expressions for the first derivatives of U_1 and U_2.

4.5 *W and its derivatives*

Let us now consider the interpolative scheme used to express the quantities

$$W, \quad \frac{\partial W}{\partial \xi_1}, \quad \frac{\partial W}{\partial \xi_2}, \quad \frac{\partial^2 W}{\partial \xi_1^2}, \quad \frac{\partial^2 W}{\partial \xi_1 \partial \xi_2} \quad \text{and} \quad \frac{\partial^2 W}{\partial \xi_2^2}$$

at the centroid of each area A_i as a linear combination of the discrete unknowns. The most difficult part of this task is to develop expressions for the second derivatives of W. (Expressions for the second derivatives of U_1 and U_2 are not required by the strain–displacement relations). Unfortunately, the expressions for the second derivatives of W cannot be obtained nearly so easily as were the expressions previously obtained for the first derivatives of U_1 and U_2.

The grid geometry involved in the derivation of the second derivatives of W is shown in Fig. 4. In order to simplify the algebra in the derivation the control points are identified by what may first appear as a somewhat cumbersome system of indexes. This indexing system is, however, especially suitable for the applications of Green's Theorem that are subsequently described. Each U_1, U_2 Control Point shown in Fig. 4 is identified by a single index (j) with one duplication: the U_1, U_2 Control Point (1) is the same point as U_1, U_2 Control Point (5). Each W Control Point shown in Fig. 4 is identified by a pair of indexes (j, k) with a substantial number of duplications as indicated in Fig. 4, and summarized below in equation form

$$\begin{aligned} (j, 5) &= (j, 1) \qquad \text{for } j = 1, 2, 3, 4 \\ (k, j) &= (j, k) \\ (4, 2) &= (1, 3) \end{aligned} \tag{4.3}$$

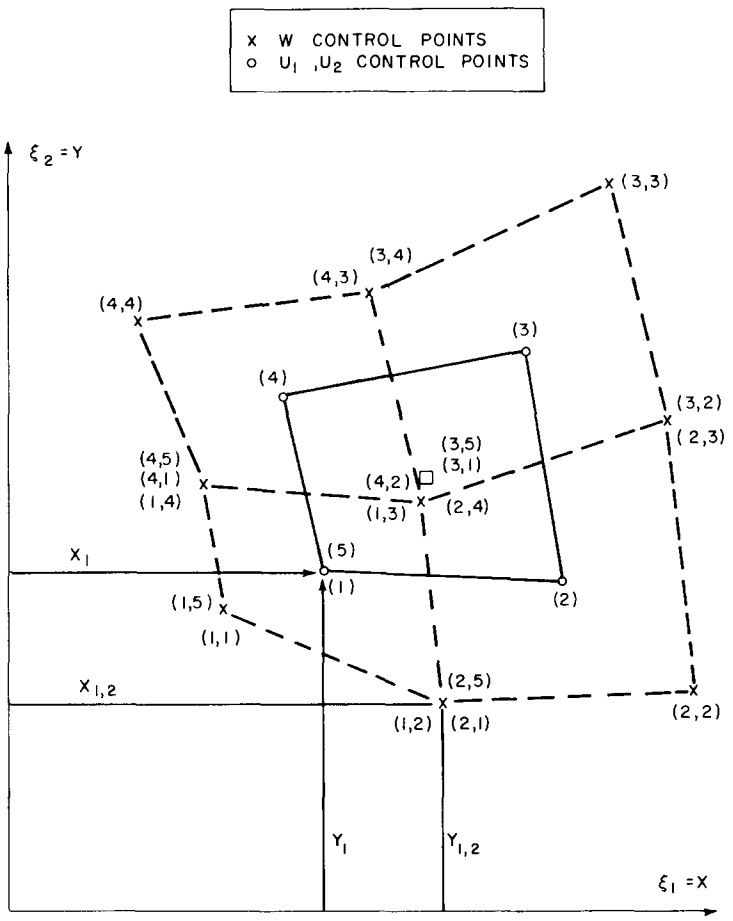

FIG. 4. Geometry for calculation of derivatives of W.

To simplify the nomenclature that follows, the independent spatial variables ξ_1 and ξ_2 are denoted by x and y respectively. The values of x and y at each control point are identified by subscripts corresponding to the indexing of each control point. Thus, the values of x and y for a W Control Point (j, k) are denoted by $x_{j,k}, y_{j,k}$ and the values of x and y for a U_1, U_2 Control Point (j) are denoted by x_j, y_j, respectively. The area of the quadrilateral formed by the U_1, U_2 Control Points shown in the figure is, as previously (Section 2), denoted by A_i. (The centroid of this area is shown by the symbol □ in Fig. 4). Each U_1, U_2 Control Point (j) shown in Fig. 4 occupies the centroid of a quadrilateral area that we denote by $\hat{A}_j$. (The symbol $\hat{}$ has been used in $\hat{A}_j$ to avoid possible ambiguity with A_i).

The interpolative scheme used to determine the second derivatives of W consists essentially of two successive applications of Green's Theorem. In order to obtain convergent expressions for the second derivatives it is necessary to assume a quadratic variation of W during the first application of Green's Theorem. The steps in the derivation are as follows:

Let us first consider a straight line segment in x, y space. Let the location of a point on the line segment be given by the path variable s, so that the beginning of the line segment is given by $s = s_a$ and the end of the line segment by $s = s_b$. The displacement component W of a point on the line segment is a function of s, denoted by $W(s)$. The Taylor series expansion of $W(s)$ about the point $s = s_a$ may be written as

$$W(s) = W(s_a) + (s - s_a)\frac{\partial W}{\partial s}\bigg|_{s_a} + \frac{(s-s_a)^2}{2}\frac{\partial^2 W}{\partial s^2}\bigg|_{s_a} + O(\delta^3) \quad \text{for } s_a \leq s \leq s_b \tag{4.4}$$

where $\delta = s_b - s_a$. By evaluating equation (4.4) at the end point $s = s_b$, one can solve for $\partial W/\partial s|_{s_a}$ and then eliminate the first derivative term in equation (4.4) to obtain the following

$$W(s) = W(s_a) + \frac{(s-s_a)}{\delta}[W(s_b) - W(s_a)] + \left[\frac{(s-s_a)^2}{2} - \frac{\delta(s-s_a)}{2}\right]\frac{\partial^2 W}{\partial s^2}\bigg|_{s_a}$$

$$+ O(\delta^3) \quad \text{for } s_a \leq s \leq s_b. \tag{4.5}$$

Integration of equation (4.5) gives

$$\int_{s_a}^{s_b} W(s)\,\mathrm{d}s = \delta\left[\frac{W(s_a) + W(s_b)}{2} - \frac{\delta^2}{12}\frac{\partial^2 W}{\partial s^2}\bigg|_{s_a}\right] + O(\delta^4) \tag{4.6}$$

Now for the straight line segment one has

$$\frac{\partial^2 W}{\partial s^2} = \left(\frac{\mathrm{d}x}{\mathrm{d}s}\right)^2\frac{\partial^2 W}{\partial x^2} + 2\left(\frac{\mathrm{d}x}{\mathrm{d}s}\right)\left(\frac{\mathrm{d}y}{\mathrm{d}s}\right)\frac{\partial^2 W}{\partial x \partial y} + \left(\frac{\mathrm{d}y}{\mathrm{d}s}\right)^2\frac{\partial^2 W}{\partial y^2}. \tag{4.7}$$

If the x, y coordinates of points $s = s_a$ and $s = s_b$ are denoted by x_a, y_a and x_b, y_b, respectively, and Δ_x and Δ_y are then defined by

$$\Delta_x = x_b - x_a \qquad \Delta_y = y_b - y_a \tag{4.8}$$

then by substitution of (4.7) into (4.6) one can obtain

$$\int_{s_a}^{s_b} W(s)\,\mathrm{d}s = \delta\left\{\frac{W(s_a) + W(s_b)}{2} - \frac{1}{12}\left[\Delta_x^2\frac{\partial^2 W}{\partial x^2}\bigg|_a + 2\Delta_x\Delta_y\frac{\partial^2 W}{\partial x \partial y}\bigg|_a + \Delta_y^2\frac{\partial^2 W}{\partial y^2}\bigg|_a\right]\right\} + O(\delta^4) \tag{4.9}$$

where the second derivatives are evaluated at point a, that is, at $x = x_a$, $y = y_a$. Because a straight line segment is involved, two of the integrals required by Green's Theorem can

be expressed in terms of the integral appearing in equation (4.9) as follows

$$\int_{s_a}^{s_b} W(s)\,dx = \left(\frac{\Delta_x}{\delta}\right)\int_{s_a}^{s_b} W(s)\,ds$$
$$\int_{s_a}^{s_b} W(s)\,dy = \left(\frac{\Delta_y}{\delta}\right)\int_{s_a}^{s_b} W(s)\,ds. \tag{4.10}$$

Before proceeding further it is convenient to define the following new symbols:

$$\left.\begin{aligned}\Delta_{x_{j,k}} &= x_{j,k+1} - x_{j,k}\\ \Delta_{y_{j,k}} &= y_{j,k+1} - y_{j,k}\end{aligned}\right\} \text{ for } \begin{cases} j = 1, 2, 3, 4\\ k = 1, 2, 3, 4\end{cases}$$
$$\left.\begin{aligned}\Delta_{x_j} &= x_{j+1} - x_j\\ \Delta_{y_j} &= y_{j+1} - y_j\end{aligned}\right\} \text{ for } j = 1, 2, 3, 4 \tag{4.11}$$
$$W_{j,k} = W(x_{j,k}, y_{j,k}).$$

Furthermore, we shall apply a subscript j to the first derivatives of W to indicate their evaluation at point x_j, y_j, and we shall apply a subscript i to the second derivatives of W to indicate their evaluation at the centroid of the area A_i.

We can now proceed by applying Green's Theorem to areas $\hat{A}_1$, $\hat{A}_2$, $\hat{A}_3$ and $\hat{A}_4$, and using equations (4.9)–(4.11) to obtain the following expressions for the first derivatives at the points x_j, y_j:

$$\left(\frac{\partial W}{\partial x}\right)_j = \frac{1}{\hat{A}_j}\sum_{k=1}^{4} \Delta_{y_{j,k}} \cdot \hat{F} + O(\Delta^2)$$
$$\left(\frac{\partial W}{\partial y}\right)_j = -\frac{1}{\hat{A}_j}\sum_{k=1}^{4} \Delta_{x_{j,k}} \cdot \hat{F} + O(\Delta^2) \quad \text{for } j = 1, 2, 3, 4 \tag{4.12}$$

where

$$\hat{F} = \frac{(W_{j,k+1} + W_{j,k})}{2} - \frac{1}{12}\left[\Delta_{x_{j,k}}^2\left(\frac{\partial^2 W}{\partial x^2}\right)_i + 2\Delta_{x_{j,k}}\Delta_{y_{j,k}}\left(\frac{\partial^2 W}{\partial x \partial y}\right)_i + \Delta_{y_{j,k}}^2\left(\frac{\partial^2 W}{\partial y^2}\right)_i\right]. \tag{4.13}$$

Two features of equations (4.12) and (4.13) merit some explanation: First, the derivation assumes that, although the grid may be nonuniform, the lengths of the line segments involved within each set of equations (4.12) are of the same order, namely, of order Δ. Secondly, there appears to be a contradiction between equation (4.13) and (4.9) concerning the location at which the second derivatives are evaluated. The technique used here was to replace each second derivative in equation (4.9) by its value at the point i (the centroid of A_i). Since the distance between each point a and point i is of order Δ, one can show from the Taylor series expansions of these second derivatives that the error thus introduced in the second derivatives is of order Δ. More importantly, it can be seen from equation (4.9) that an error of order Δ in the second derivatives will not lower the order of the error of the entire equation (4.9) because the coefficient of each second derivative term in (4.9) is proportional to Δ^3. Consequently, equations (4.12) are correct to the order shown. The importance of evaluating all second derivatives at point i will become more apparent in the next step.

We next apply Green's Theorem to the area A_i, (assuming a linear variation of the first derivatives) to give†:

$$\left(\frac{\partial^2 W}{\partial x^2}\right)_i = \frac{1}{A_i}\sum_{j=1}^{4}\frac{\Delta_{y_j}}{2}\left[\left(\frac{\partial W}{\partial x}\right)_{j+1}+\left(\frac{\partial W}{\partial x}\right)_j\right]+O(\Delta)$$

$$\left(\frac{\partial^2 W}{\partial x \partial y}\right)_i = \frac{1}{A_i}\sum_{j=1}^{4}\frac{\Delta_{y_j}}{2}\left[\left(\frac{\partial W}{\partial y}\right)_{j+1}+\left(\frac{\partial W}{\partial y}\right)_j\right]+O(\Delta) \tag{4.14}$$

$$\left(\frac{\partial^2 W}{\partial y^2}\right)_i = -\frac{1}{A_i}\sum_{j=1}^{4}\frac{\Delta_{x_j}}{2}\left[\left(\frac{\partial W}{\partial y}\right)_{j+1}+\left(\frac{\partial W}{\partial y}\right)_j\right]+O(\Delta).$$

The equations which result from substitution of equations (4.12) and (4.13) into equations (4.14) may be put in the following matrix form

$$\hat{\mathbf{d}} = \hat{\mathbf{B}}\hat{\mathbf{d}} + \hat{\mathbf{C}}\hat{\mathbf{w}} + O(\Delta) \tag{4.15}$$

in which

$$\hat{\mathbf{d}} = \begin{Bmatrix} \left(\frac{\partial^2 W}{\partial x^2}\right)_i \\ \left(\frac{\partial^2 W}{\partial x \partial y}\right)_i \\ \left(\frac{\partial^2 W}{\partial y^2}\right)_i \end{Bmatrix} \qquad \hat{\mathbf{w}} = \begin{Bmatrix} W_{1,1} \\ W_{1,2} \\ W_{1,3} \\ W_{1,4} \\ W_{2,2} \\ W_{2,3} \\ W_{3,3} \\ W_{3,4} \\ W_{4,4} \end{Bmatrix}. \tag{4.16}$$

The matrices $\hat{\mathbf{B}}$ and $\hat{\mathbf{C}}$ are functions only of the geometric quantities A_i, $\hat{A}_j$, Δ_{x_j}, Δ_{y_j}, $\Delta_{x_{k,j}}$ and $\Delta_{y_{k,j}}$. In performing the algebraic manipulations required to obtain the elements of $\hat{\mathbf{B}}$ and $\hat{\mathbf{C}}$ one must take into account the previously described duplications in the indexing system. [See equations (4.3) and the paragraph preceding equations (4.3)]. Matrix $\hat{\mathbf{B}}$ contains three rows and three columns; matrix $\hat{\mathbf{C}}$ contains three rows and nine columns.

The final task is to solve equation (4.15) for $\hat{\mathbf{d}}$ as follows

$$\hat{\mathbf{d}} = (\mathbf{I}-\hat{\mathbf{B}})^{-1}\hat{\mathbf{C}}\hat{\mathbf{w}} + O(\Delta) \tag{4.17}$$

where $\mathbf{I}$ represents a 3×3 identity matrix. Thus the second derivatives, $\hat{\mathbf{d}}$, are determined to within an error of order Δ. There naturally arises the question of whether or not the matrix $(\mathbf{I}-\hat{\mathbf{B}})$ may be singular. On the basis of experience to date, it appears that matrix $(\mathbf{I}-\hat{\mathbf{B}})$ will

† The second of equations (4.14) is based on the discrete analog of

$$\frac{\partial^2 W}{\partial x \partial y} = \frac{\partial}{\partial x}\left(\frac{\partial W}{\partial y}\right).$$

Recent calculations suggest that greater accuracy may be obtained by using the discrete analog of

$$\frac{\partial^2 W}{\partial x \partial y} = \frac{1}{2}\frac{\partial}{\partial x}\left(\frac{\partial W}{\partial y}\right)+\frac{1}{2}\frac{\partial}{\partial y}\left(\frac{\partial W}{\partial x}\right).$$

not be singular except possibly in certain special cases of severely distorted grids. (For severely distorted grids, one usually expects numerical difficulties in almost any numerical method).

Finally, some other aspects of the procedure used to obtain the second derivatives merit comment. First, for the special case in which the W Control Points form four parallelograms one has

$$\left.\begin{aligned} \Delta_{x_{j,r}} &= -\Delta_{x_{j,r+2}} \\ \Delta_{y_{j,r}} &= -\Delta_{y_{j,r+2}} \end{aligned}\right\} \quad \begin{aligned} j &= 1,2,3,4 \\ r &= 1 \text{ and } 2. \end{aligned} \tag{4.18}$$

and consequently $\hat{\mathbf{B}} = 0$, thus rendering the matrix $(\mathbf{I}-\hat{\mathbf{B}})$ obviously nonsingular. (One may also have $\hat{\mathbf{B}} = 0$ in certain other special situations when the grid arrangements possess sufficient symmetries). Secondly, if, as one increases the number of control points, the grid is successively refined so that as $\Delta \to 0$ the quadrilaterals approach parallelograms in the manner prescribed by the following equations

$$\left.\begin{aligned} \Delta_{x_{j,r}} &= -\Delta_{x_{j,r+2}}[1+O(\Delta)] \\ \Delta_{y_{j,r}} &= -\Delta_{y_{j,r+2}}[1+O(\Delta)] \end{aligned}\right\} \quad \begin{aligned} j &= 1,2,3,4 \\ r &= 1 \text{ and } 2 \end{aligned} \tag{4.19}$$

then the elements of $\hat{\mathbf{B}}\hat{\mathbf{d}}$ are of order Δ, the same order as the error in equation (4.15), and may be neglected in the computation.

Once the second derivatives of W have been evaluated at the centroid of an area A_i, the values of W and its first derivatives at the centroid may also be obtained quite easily by using the appropriate Taylor Series and the first derivatives of W evaluated at "U_1, U_2 Control Points" from equations (4.12).

4.6 *Interpolations required by boundary conditions*

For force-type boundary conditions (involving the specification of N_1, N_2, N_n or M_s) it is necessary to construct matrix equations (2.22b) and (2.22c); for displacement-type boundary conditions (involving the specification of U_1, U_2, W or ϕ_s) it is necessary to construct matrix equation (3.1). Unlike the usual finite difference methods, this method, by virtue of its basis on a variational principle, does not require that N_1, N_2, N_n or M_s be expressed as functions of the discrete displacements. [N_1, N_2, N_n and M_s are specified externally applied loads (or moments)]. All that is required is the computation of the work done by the specified values of N_1, N_2, N_n and M_s. The work done by these loads (or moments) thus only involves interpolations of U_1, U_2, W or ϕ_s along the boundary. Therefore, unlike in the usual finite difference method, it is not necessary to evaluate first derivatives of U_1 and U_2 or second derivatives of W at the boundary. Indeed, backwards differences, which create difficulties in the usual finite difference method, are *totally absent* from this method. Furthermore, because of the manner in which the control points are positioned with respect to the boundary, the required interpolations of U_1, U_2, W and ϕ_s are very simple.

The positioning of U_1, U_2 Control Points directly on the boundary (see Figs. 3 and 5) simplifies the generation of the equations associated with the specification of U_1 (or N_1) and U_2 (or N_2). Thus boundary conditions specifying the values of U_1 or U_2 on the boundary can be stated in terms of the discrete unknowns [as required by equation (3.1)] without any interpolation whatsoever: one can directly specify the value of a particular discrete unknown

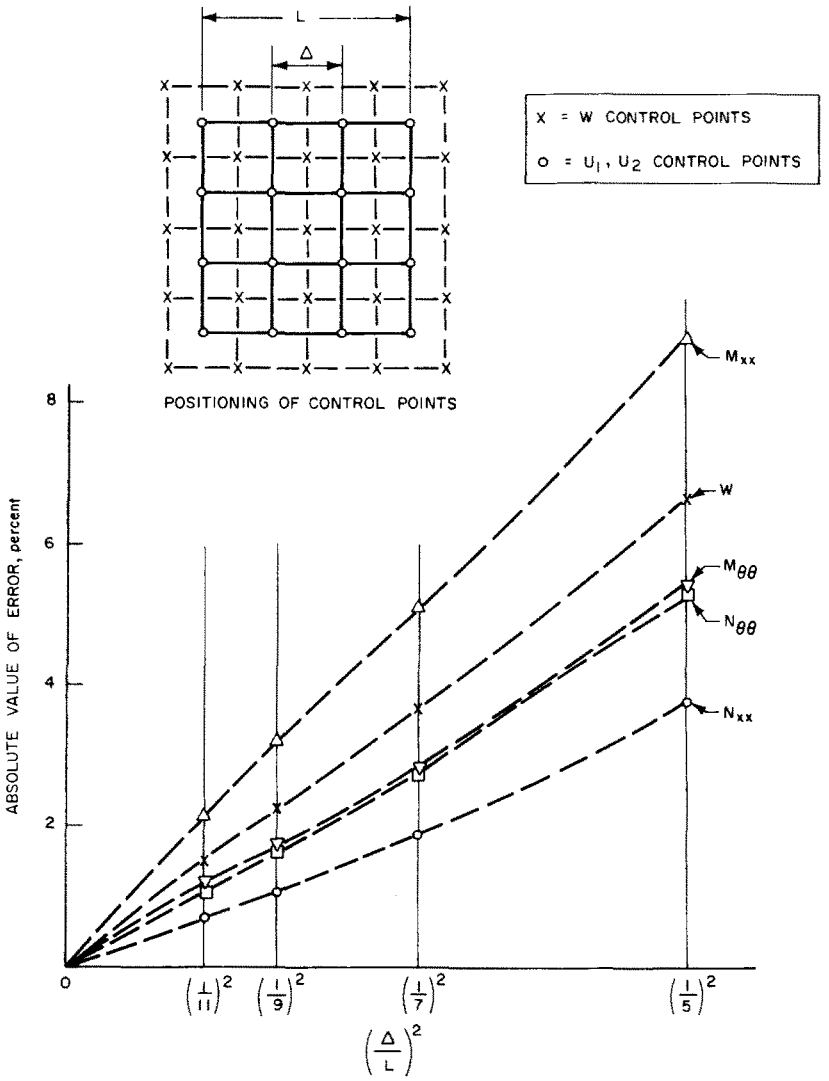

FIG. 5. Convergence of results at midpoint of rectangular cylindrical shell panel.

U_1 or U_2 at its position on the boundary. A simple linear interpolation of U_1 or U_2 along the boundary provides the required values at the centroid of each length s_j for the evaluation of the work done by the external loads N_1 and N_2.

The positioning of W Control Points in pairs (see Figs. 3 and 5) so that the boundary passes through the midpoint between each pair similarly simplifies the generation of those equations associated with the specification of W (or N_n) and ϕ_s (or M_s). By this positioning, the values of both W and the normal derivative of W at each midpoint are easily expressed (to order Δ^2) as a linear combination of two discrete values of W, i.e. the values of W at the adjacent pair of W Control Points. Thus boundary conditions specifying the values of W or the normal derivative of W are stated directly for each such midpoint on the boundary by an algebraic equation [as required by equation (3.1)] which involves only two discrete unknown values of W. Boundary conditions specifying the values of ϕ_s (ϕ_s involves both

the normal derivative of W and values of U_1 and/or U_2) are also stated at each such midpoint on the boundary by linearly interpolating the required values of U_1 and/or U_2 along the boundary†. A simple linear interpolation of these values of W and ϕ_s along the boundary provides the required values at the centroid of each length s_j for the evaluation of the work done by the external normal load N_n and the external moment M_s.

In each case, the treatment of boundary conditions described above leads to truncation errors of order Δ^2 or higher.

5. COMPARISON WITH FINITE ELEMENT METHOD

Although a detailed comparison of the method presented here with the finite element method is beyond the scope of this paper, it is nevertheless useful to make a brief comparison between these two methods. Because of the considerable variation among finite element methods themselves, and because of the broad range of physical problems which may be treated by these methods, this brief comparison can serve only as a general guide. In the paragraphs that follow, comparative discussions of five important aspects of each method are presented.

We begin by considering the relative ease in generating the mesh. Except in the vicinity of boundaries both methods present approximately the same ease with respect to mesh generation. As previously described, this method requires the proper positioning of both U_1, U_2 Control Points and W Control Points at (or near) a boundary, whereas the corresponding nodal positioning required by the finite element methods is generally somewhat simpler. Nevertheless, the automatic mesh generation scheme used in this work allows all control points (both in the interior and near the boundaries) to be easily positioned.

Next, we look at the relative ease in generating the linear algebraic equations. Because the present method is based on an evaluation of quantities at centroidal points, the necessity of performing numerical integrations over each "element", as usually encountered in the finite element methods, is avoided. This not only results in shorter computation times (for a given number of unknowns) but it also simplifies the writing and checking of the computer code.

Thirdly, we consider the relative ease in imposing boundary conditions. Once the appropriate mesh has been generated most boundary conditions can be imposed as easily as in the finite element method. Admittedly, the present method involves fictitious W Control Points outside of each boundary; however, there is considerable precedent available for the use of fictitious points and, indeed, they can be positioned automatically with virtually the same ease as the other points. The interpolations required for certain displacement boundary conditions, such as the specification of a rotation but not a displacement, generally present more algebraic complications than their finite element counterparts.

Another important aspect involves the relative topologies of the coefficient matrix. It is difficult to make a meaningful comparison of the relative topologies because of the different selection of unknowns and the different positioning of control points (nodes) used in this method as compared with the finite element methods. However, a reasonable basis for comparison would be obtained if we were to compare the matrices generated by each

† For boundary conditions specifying W, the normal derivative of W, or ϕ_s, the partitioning of $\mathbf{u}$ (see Section 3) is carried out so that values of W at the fictitious points (outside the boundary) are assigned to $\mathbf{u}_b$.

method for a rectangular grid of mesh points in which the finite element nodes occupy the same grid of points as the W Control Points of this method. The statements which follow apply to such a rectangular grid with a large number of points. Typical finite element formulations carry five unknowns per node (three displacement components and two rotation components) with a resulting connectivity such that each equation involves three rows of nodes. On the basis of comparison defined above, corresponding to each "finite element node" the present method employs three unknowns (three displacement components) with a resulting connectivity such that each equation involves five rows of these "finite element nodes." Consequently, for a large number of unknowns the relative band widths of the matrices are essentially 10/12 (finite element/present method). However, because the total number of unknowns is less in the present method, the standard modified elimination algorithm, which takes advantage of the sparseness of the matrix, will nevertheless solve the matrix equations slightly faster for the present method than for the finite element method.

Finally we turn our attention to limitations of the method. From a practical point of view the primary differences between this method and the finite element method involve the treatment of rapid property variations and discontinuities. As previously shown in the derivation, this method is based on the assumption that the stresses, strains, displacements and external loadings vary smoothly in the interior of the shell away from the boundaries. Consequently, if the geometric and material properties of the shell vary rapidly we would expect the convergence of this method to be slower than the convergence of the finite element method. This is part of the price to be paid for the centroidal approximation (used in this method) in return for the greater ease in generating the linear algebraic equations. In the case of discontinuous properties, such as an abrupt change of shell thickness, it would be necessary to modify the present method† whereas the finite element method could be used without special modification.

6. RESULTS

6.1 *Rectangular cylindrical shell panel*

A simple example that illustrates the convergence of the method is the following problem of a rectangular cylindrical shell panel. Pertinent parameters for the cylindrical shell are obtained from the parameters for the general shell by setting

$$\begin{aligned} &\xi_1 = x \qquad U_1 = U \qquad R_1 = \infty \qquad \alpha_1 = 1 \\ &\xi_2 = \theta \qquad U_2 = V \qquad R_2 = R \qquad \alpha_2 = R. \end{aligned} \tag{6.1}$$

In addition, the subscripts x and θ will be used in place of 1 and 2, respectively. The boundary conditions for the problem considered here are given by

$$\begin{aligned} &M_{xx} = N_{xx} = W = V = 0 \quad \text{for } 0 \le \theta \le \bar{\theta} \quad \begin{cases} x = 0 \\ x = L \end{cases} \\ &M_{\theta\theta} = N_{\theta\theta} = W = U = 0 \quad \text{for } 0 \le x \le L \quad \begin{cases} \theta = 0 \\ \theta = \bar{\theta}. \end{cases} \end{aligned} \tag{6.2}$$

† Such a modification is clearly possible; it would require special treatment near lines along which the discontinuities are found.

The loading is given by

$$f_n = \sin \pi \frac{x}{L} \sin \pi \frac{\theta}{\bar{\theta}}$$
$$f_1 = f_2 = 0. \tag{6.3}$$

The shell is assumed to be isotropic, single-layered and of uniform thickness. This particular problem was chosen because it has an exact solution given by

$$U = \hat{U} \cos \pi \frac{x}{L} \sin \pi \frac{\theta}{\bar{\theta}}$$
$$V = \hat{V} \sin \pi \frac{x}{L} \cos \pi \frac{\theta}{\bar{\theta}} \tag{6.4}$$
$$W = \hat{W} \sin \pi \frac{x}{L} \sin \pi \frac{\theta}{\bar{\theta}}$$

where $\hat{U}$, $\hat{V}$ and $\hat{W}$ are constants dependent upon h, R, ν, E, L and $\bar{\theta}$. Numerical values for the case considered here are as follows: $h = 1{\cdot}0$, $R = L = 25{\cdot}0$, $\nu = 0{\cdot}3$, $E = 10^7$ psi and $\bar{\theta} = 1$ rad. For these numerical values both bending and stretching play important roles in the response of the shell. Numerical results, expressed in terms of per cent error from the exact solution (obtained from Sanders' equations [12]) are shown in Fig. 5. This figure, which shows the non-zero displacement and generalized stress components, illustrates the convergence of the method.

6.2 *Closed cylindrical shell with circular hole*

A more complicated example is that of a closed cylindrical shell with a circular hole. We consider the case in which a uniform tensile force is applied at the ends of the cylinder. The shell is assumed to be isotropic, single-layered and of uniform thickness. Consequently, there exist two planes of symmetry and, therefore, the problem can be solved by considering the portion of shell shown in Fig. 3. This figure shows the arrangement of control points actually used to obtain the results shown in Table 2. The control points are arranged so as to provide the desired concentration of points in the vicinity of the hole. The physical

TABLE 2. COMPARISON OF RESULTS: CYLINDER WITH CIRCULAR HOLE

	σ_{xx}/σ_T at point "A" in Fig. 3 (σ_T = tensile stress applied at ends of shell)	
	At shell middle surface	At inner surface
Present method with 753 unknowns† (Grid shown in Fig. 3)	3·603	4·096
Reference 11	3·658	4·180
Per cent difference	1·5%	2·0%

† The computer time for this entire problem was 13·6 min on the IBM 360/75.

parameters defining the problem considered are: $R = 10{\cdot}0$ in., $h = 0{\cdot}1$ in., a (radius of hole) $= 1{\cdot}1002$ in., L_s (the half-length of the shell) $= 30$ in., $\nu = 0{\cdot}3$ and $E = 10^7$ psi. This particular problem was solved analytically by Eringen, Naghdi and Thiel [19] and comparisons of the results are shown in Table 2. The stresses listed in Table 2 are the maximum stresses in the shell; these maximum stresses occur at the edge of the hole (point "A" in Fig. 3). In the present method the stresses at the edge of the hole are obtained by interpolation from the stresses at nearby points. The agreement is excellent, particularly in view of the fundamental difference between the two methods of solution.

A contour plot showing the distribution of σ_{xx}/σ_T for this numerical example is given in Fig. 6.

This method has also been applied to various other cutout problems. Shells with other hole shapes have been analyzed and studies have also been conducted to determine suitable schemes for locally thickening a shell in the vicinity of a hole.

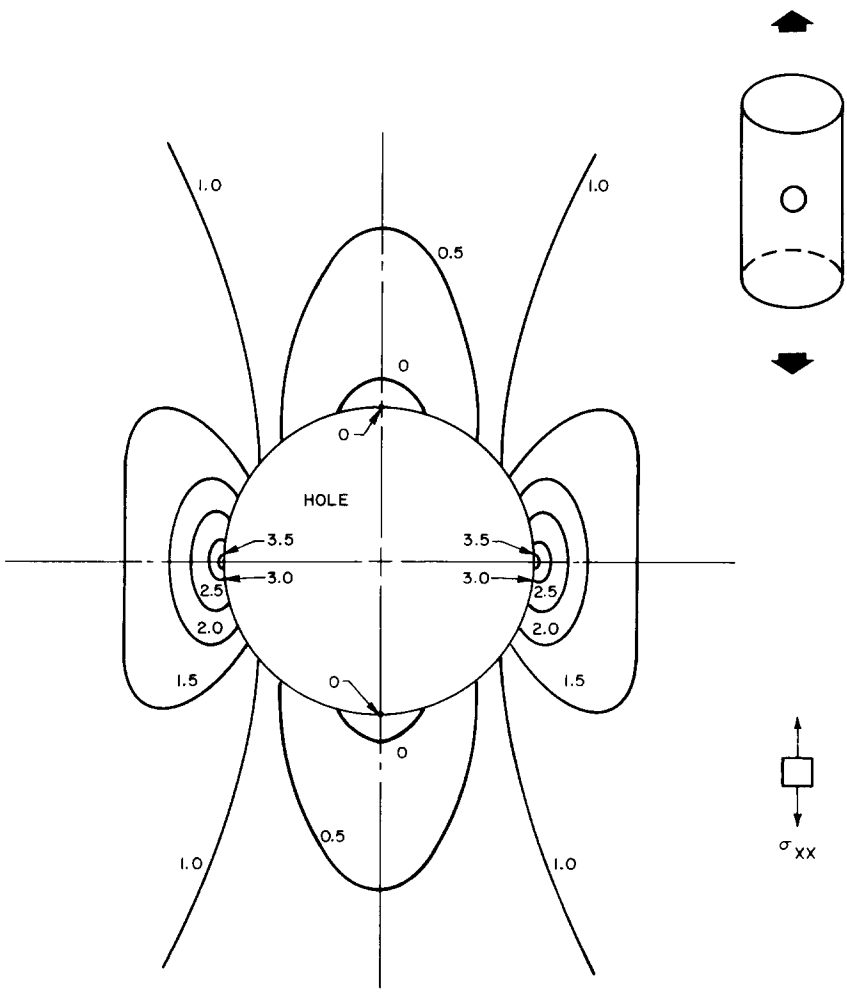

FIG. 6. Plot of σ_{xx}/σ_T at shell middle surface for cylindrical shell subjected to axial tensile stress σ_T.

7. CONCLUDING REMARKS

A difference-based variational method for analyzing a general class of two-dimensional shell problems has been presented. The method is essentially a highly organized adaptation of the variational method for setting up difference operators. The systematic development for the general shell problem presented in this paper leads to a discretized potential energy function with well-defined truncation errors and to a symmetric stiffness matrix. The method preserves the relative advantage of the variational approach over the usual finite difference method with respect to force-type boundary conditions, namely, the advantage of not necessitating the use of backwards differences. The computer coding required by this method is relatively straightforward and does not involve the tedious numerical integrations found in the corresponding finite element methods. The effectiveness and versatility of this method are illustrated by the presentation of results for two examples: a panel problem and a cutout problem. Other problems, such as problems involving a local thickening in the vicinity of a cutout, have also been investigated by this method. The work described here was limited to linear elastic small displacements, but this limitation is not inherent in the method itself, which possesses considerably broader applicability.

REFERENCES

[1] R. COURANT, K. FRIEDRICHS and H. LEWY, Über die partiellen Differenzengleichungen der mathematischen Physik. *Math. Ann.* **100**, 32–74 (1928).
[2] G. E. FORSYTHE and W. R. WASOW, *Finite-Difference Methods for Partial Differential Equations*. Wiley (1960).
[3] D. GREENSPAN, A numerical approach to biharmonic problems. *Comput. J.* **10**, 198–201 (1967).
[4] K. S. HAVNER and E. L. STANTON, On energy-derived difference equations in thermal stress problems. *J. Franklin Inst.* **284**, 127 (1967).
[5] D. S. GRIFFIN and R. B. KELLOGG, A numerical solution for axially symmetric and plane elasticity problems. *Int. J. Solids Struct.* **3**, 781 (1967).
[6] K. S. HAVNER, On convergence of iterative methods in plastic strain analysis. *Int. J. Solids Struct.* **4**, 491 (1968).
[7] K. S. HAVNER, On the formulation and iterative solution of small strain plasticity problems. *Q. Appl. Math.* **23**, 323 (1966).
[8] S. UTKU, Stiffness matrices for thin triangular elements of nonzero gaussian curvature. *AIAA Jnl* **5**, 1659–1667 (1967).
[9] R. W. CLOUGH and C. P. JOHNSON, A finite element approximation for the analysis of thin shells. *Int. J. Solids Struct.* **4**, 43–60 (1968).
[10] J. H. ARGYRIS and D. W. SCHARPF, The sheba family of shell elements for the matrix displacement method. *J. R. aeronaut. Soc.* **72**, 873–883 (1968).
[11] G. A. WEMPNER, J. T. ODEN and D. A. KROSS, Finite-element analysis of thin shells. *J. Engng. Mech. Div. Am. Soc. civ. Engrs* **94**, 1273 (1968).
[12] J. L. SANDERS, JR., An improved first-approximation theory for thin shells. NASA Rept. 24 (June 1959).
[13] P. TONG and T. H. H. PIAN, The convergence of finite element method in solving linear elastic problems. *Int. J. Solids Struct.* **3**, 865–879 (1967).
[14] L. COLLATZ, *The Numerical Treatment of Differential Equations*. Springer (1966).
[15] D. GREENSPAN, On the numerical solution of problems allowing mixed boundary conditions. *J. Franklin Inst.* **227**, 11 (1964).
[16] K. S. HAVNER, Finite-difference solution of two variable thermal and mechanical deformation problems. *J. Spacecr. & Rockets* **2**, 542 (1965).
[17] D. S. GRIFFIN and R. S. VARGA, Numerical solution of plane elasticity problems, *J. Soc. ind. appl. Math.* **11**, 1046 (1963).
[18] R. S. VARGA, *Matrix Iterative Analysis*, Chapter 6. Prentice-Hall (1962).
[19] A. C. ERINGEN, A. K. NAGHDI and C. C. THIEL, State of stress in a circular cylindrical shell with a circular hole. *Weld. Res. Coun. Bull.* **102** (1965).

(*Received* 28 *April* 1969; *revised* 8 *September* 1969)

Абстракт—На основе конечных разностей в работе описывается вариационный метод в сцелью анализа общего класса двухмерных задач, включая оболочки с очертанием. По существу, метод является адаптацией вариационного метода для установления разностных операторов. Даются результаты из двух примерных задач и иллюстрируется эффективность метода. Несмотря на то, что метод имеет широкую применимость, эта работа ограничается только тематикой, касающейся линейных, упругих, статических деформаций тонких оболочек.